

MS-Mix: An Adaptive Emotion-Sensitive Mixup Framework for Multimodal Sentiment Analysis

Hongyu Zhu^a, Lin Chen^{a,*}, Xin Jin^b, Mounim A. El-Yacoubi^c, Mingsheng Shang^{a,*}

^aChongqing Institute of Green Intelligent Technology, Chinese Academy of Sciences; Chongqing School, University of Chinese Academy of Sciences, 400714, Chongqing, China

^bSchool of Engineering, Westlake University, Zhejiang, China

^cTelecom SudParis, Institute Polytechnique de Paris, Palaiseau, France

Abstract

Multimodal Sentiment Analysis (MSA) integrates complementary features from text, video, and audio to achieve robust emotion understanding. Yet, models for this task suffer from severe data scarcity and high annotation costs. This severely restricts their practical engineering applications. Although Mixup-based augmentation improves generalization in unimodal settings, its naive application to MSA often produces semantically inconsistent mixtures and amplified label noise due to random sample mixing and fixed mixing ratios that ignore emotional semantics. To overcome these issues, we propose MS-Mix, an adaptive, emotion-sensitive augmentation framework that automatically optimizes sample mixing in multimodal settings. The key components of MS-Mix include: (1) a Sentiment-Aware Sample Selection strategy that filters incompatible pairs by measuring semantic similarity in the latent space, preventing mixtures of contradictory emotions. (2) a Sentiment Intensity Guided module using multi-head self-attention, that dynamically computes modality-specific mixing ratios conditioned on emotional salience. (3) a Sentiment Alignment Loss based on Kullback-Leibler divergence that regularizes the model by aligning predicted sentiment distributions across modalities with ground-truth labels, improving discrimination and consistency. Extensive experiments on three benchmark datasets with six state-of-the-art backbones confirm that MS-Mix consistently outperforms existing methods, thereby improving the robustness and practical applicability of MSA in engineering contexts. The source code is available at an anonymous link: <https://anonymous.4open.science/r/MS-Mix-review-0C72>.

Keywords: Affective computing, Multimodal sentiment analysis, Data augmentation, Regularization

1. Introduction

The perception and understanding of human emotions by Artificial Intelligence (AI) are of great significance for technologies such as human-computer interaction [1], and multimedia computing [2]. Multimodal Sentiment Analysis (MSA) has emerged as a critical research frontier in this endeavor [3, 4, 5, 6, 7]. MSA aims to integrate and interpret complementary

*Lin Chen and Mingsheng Shang are the corresponding authors.

Email addresses: zhuhongyu@cigit.ac.cn (Hongyu Zhu), chenlin@cigit.ac.cn (Lin Chen)

emotional features from textual, acoustic, and visual modalities to achieve a more robust and accurate understanding of sentiment [8]. The significance of MSA is underscored by its wide-ranging applications, including but not limited to opinion mining on social media [9], empathetic chatbot design [10], and mental health assessment [11]. By moving beyond unimodal analysis, MSA can capture the complex, often incongruent nature of human affective expression, thereby providing a more holistic view of sentiment.

Benefiting from rapid advances in Deep Learning (DL), the field of MSA has witnessed substantial progress in developing neural architectures. Techniques such as cross-modal transformers [12] and advanced fusion mechanisms [6] have demonstrated remarkable capability in modeling inter-modal interactions and extracting discriminative features. Nevertheless, despite these architectural advancements, the performance of data-driven DL models remains fundamentally constrained by the scale and quality of annotated data [13]. This data scarcity often results in overfitting and limited generalization ability [14]. Furthermore, constructing MSA datasets is costly, as it requires the collection of reliable, human-annotated multimodal sentiment datasets. Above all, these issues severely restrict the practical engineering applications of MSA.

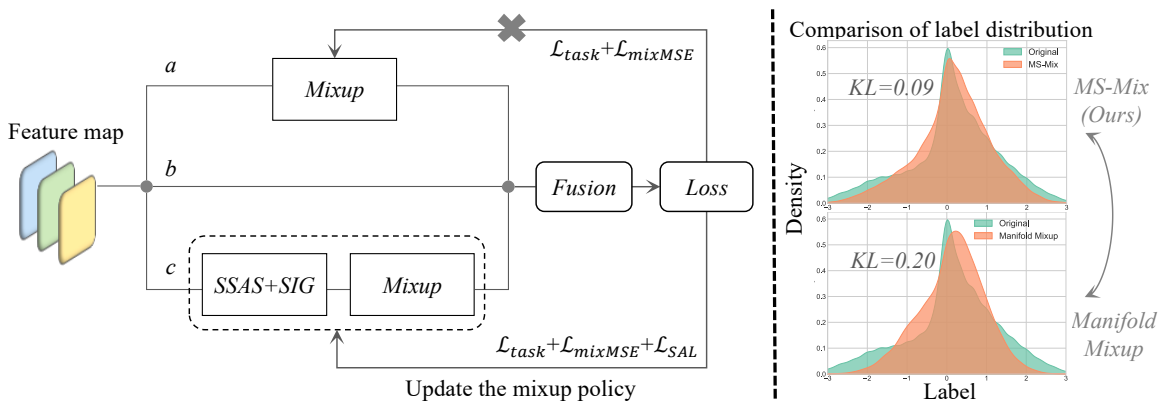


Figure 1: The differences between MS-Mix and traditional mixup methods represented by Manifold Mixup [13]. **Left:** a. The traditional methods employ random sampling and an offline optimization of mixing ratios. b. Backbone. c. MS-Mix. **Right:** MS-Mix can generate augmented samples that better align with the original label distribution.

To mitigate data scarcity, the mixup strategy, a data augmentation technique, was introduced to generate virtual training samples by convexly interpolating between original data points and their corresponding labels [13]. However, existing offline methods, including general domain techniques such as CutMix [15] and SaliencyMix [16], as well as multimodal specific approaches like *PowMix* [17] and *MultiMix* [18], often depend on randomly paired samples and offline optimization strategies, thereby neglecting the underlying emotional semantics. This may result in the blending of semantically inconsistent samples, *e.g.*, combining a positive and a negative sample can introduce semantic confusion and label mismatch. Moreover, these methods typically use fixed or uniformly distributed mixing ratios, which do not adapt to the varying emotional intensities across modalities. As a consequence, the quality and efficacy of the augmented data are substantially compromised.

To address these limitations, we propose MS-Mix, a novel, adaptive data augmentation framework designed for multimodal sentiment analysis. As shown in Fig. 1, we have visual-

ized the distribution of the generated labels, and MS-Mix has a lower Kullback- Leibler (KL) divergence. It can be observed that the label distribution generated by MS-Mix is closer to the real situation. Our method introduces three key innovations to ensure semantically consistent and high-quality sample generation: (1) We design a Sentiment-Aware Sample Selection (SASS) strategy that leverages semantic similarity in the latent space to filter out incompatible pairs, thereby preventing the mixture of samples with contradictory emotions. (2) We introduce a Sentiment Intensity Guided (SIG) mixing module to dynamically determine the mixing ratio across modalities, which leverages a multi-head self-attention mechanism to predict modality-specific mixing ratios conditioned on sentiment salience, thereby enabling more fine-grained and context-aware fusion. (3) We introduce a Sentiment Alignment Loss (SAL) to align the predicted sentiment distribution with the ground-truth labels. The SAL acts as a regularization term, enhancing the backbone network’s discriminative power and improving the consistency of representations from augmented samples. Experimental results on real-world MSA datasets show that MS-Mix significantly outperforms existing methods across multiple baselines and backbone architectures. The main contributions of this paper are summarized as follows:

- We design a SASS strategy that leverages semantic similarity in the latent space to filter out incompatible sample pairs, effectively preventing mixtures of samples with contradictory emotions.
- We introduce a SIG mixing module, implemented via a multi-head self-attention mechanism, to dynamically determine modality-specific mixing ratios based on emotional salience.
- We propose SAL, a Kullback-Leibler divergence-based regularization that aligns predicted sentiment distributions with ground-truth labels, thereby enhancing both model discrimination and consistency.

The remainder of this paper is organized as follows: Section 2 reviews related works. The proposed MS-Mix method is detailed in Section 3. The experimental results and visualizations are presented in Section 4, and the conclusions are provided in Section 5.

2. Related Work

2.1. Multimodal Sentiment Analysis

Sentiment analysis systems are divided into single-modal systems and multimodal systems. Compared with single-modal systems, which analyze sentiment using a single data source, MSA systems can leverage complementary information across multiple modalities, such as text, video, and audio, thereby providing a more comprehensive approach to sentiment analysis [19]. For instance, Cimtay et al. [20] achieved emotion recognition by extracting data features from Galvanic Skin Response (GSR), Electroencephalogram (EEG), and facial expressions. Prior research in MSA has predominantly focused on improving two main paradigms: feature-fusion strategy-centric [21, 22, 23, 12, 24, 6] and feature-encoder method-centric [25, 26, 27, 5] approaches.

Fusion strategy-centric approaches in MSA primarily focused on designing effective fusion strategies to integrate features from different modalities. Zadeh et al. [21] introduced the

Tensor Fusion Network (TFN), which explicitly models intermodal interactions via the 3-fold Cartesian product. Building on this work, Z. Liu et al. [22] proposed Low-rank Multimodal Fusion (LMF), an efficient approach that improves computational performance through parallel tensor and weight decomposition. By leveraging modality-specific low-rank factors, LMF achieves effective multimodal fusion with significantly reduced computational cost. MuIT [12] incorporates cross-modal attention, explores long-range dependencies among cross-modal elements in multimodal datasets, and achieves multimodal fusion across unaligned datasets. A recent advancement in MSA is the attempt to decouple the features into shared and unique information. For instance, Li et al. [28] proposed a Decoupled Multimodal Distillation (DMD) method that distills cross-modal knowledge in decoupled feature spaces and alleviates the inherent multimodal heterogeneity. The Global Local Modal (GLoMo) [6] Fusion framework integrates multiple local representations within each modality and effectively combines local and global information.

In feature encoder-centric approaches, the primary objective is to improve the feature representation for each modality. Yang et al. [26] conceptualize multimodal representation learning as a form of domain adaptation, employing adversarial learning to model both modality-invariant and modality-specific subspaces within multimodal fusion. To address the challenge of multimodal heterogeneity in MSA, Li et al. [27] conceptualized the learning process of each modality as a set of sub-tasks and introduced a novel Multi-Task Momentum Distillation (MTMD) method. This approach effectively reduces the discrepancies between modalities and enhances representation consistency. Furthermore, to suppress sentiment-irrelevant and conflicting information across modalities, in recent work, Zhang et al. [5] proposed the Adaptive Language-guided Multimodal Transformer (ALMT), which learns a unified hypermodality representation guided by language at multiple scales.

Despite these advancements, MSA systems remain constrained by the scarcity and high annotation costs of multimodal data, which often lead to overfitting and limited generalization [18, 17]. This highlights the need for effective data augmentation techniques specifically designed for multimodal emotional data.

2.2. Mixup-based Augmentation

To mitigate data scarcity and improve generalisation, data augmentation techniques, particularly Mixup and its variants, have been widely adopted in DL [29, 30, 31, 32, 33]. The original Mixup method [13] operates in the input space by generating virtual samples through linear interpolation between two randomly selected data points and their corresponding labels. This simple yet effective strategy encourages models to behave linearly across classes and improves robustness. Subsequent extensions, such as Manifold Mixup [34], generalize the interpolation operation to hidden representations, further enhancing the smoothness of decision boundaries. Similarly, in the latent space, the Mixup-Transformer [35] encodes a sentence using a Transformer and then linearly interpolates the representations to generate mixed samples for classification. In the latest work, AdvMixUp [33] introduces a sample-dependent, feature-level interpolation mask generated by a compact Mask Generator, optimized via adversarial training (min-max framework) to produce challenging "hard" mixed samples near decision boundaries. Recent state-of-the-art approaches [30, 31, 33] that use mixing strategies no longer rely on manually designed rules based on prior knowledge or

saliency information, but instead adaptively generate mixed samples using learnable mixing ratios and feature representations in an end-to-end manner.

In the multimodal domain, several works have extended Mixup to leverage cross-modal interactions. For instance, MultiMix [18] performs independent Mixup operations within each modality and integrates the augmented representations through late fusion. VLMixer [36] integrates cross-modal CutMix [15] with contrastive learning to convert uni-modal text inputs into multi-modal representations of text and image, thereby improving instance-level alignment across modalities. To enhance robustness against missing modalities, Lin et al. [37] proposed Multi-Modal Mixup (M^3 ixup), which extends mixup to both representation and contrastive loss levels to improve cross-modal alignment and capture of dynamics. More recently, as an improvement of MultiMix, \mathcal{P} owMix [17] introduced a weight-aware mixing strategy that dynamically modulates mixing coefficients based on the estimated importance of each modality, enabling more flexible and effective multimodal augmentation.

However, most existing methods rely on random sampling and offline mixing, which overlook the semantic structure and emotional coherence of multimodal data. This often results in semantically inconsistent mixtures, such as mixing samples with opposing emotions, which introduces label noise and hinders model performance. These limitations underscore the need for more semantically aware and adaptively controlled mixing strategies tailored to multimodal sentiment analysis. Therefore, we propose MS-Mix, a novel mixup method that effectively avoids the mixing of contradictory emotions and adaptively generates discriminative multimodal emotional features.

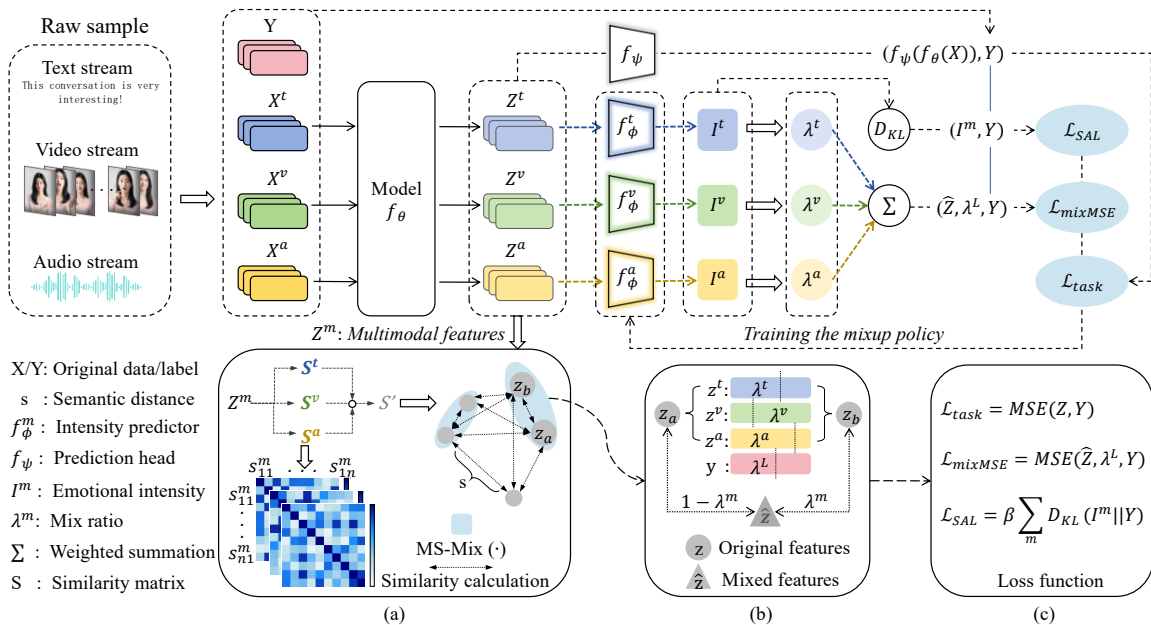


Figure 2: An overview of the proposed MS-Mix framework. (a) The SASS strategy computes the emotional semantic distance between samples. (b) The SIG module performs adaptive mixing of sample pairs with similar emotional semantics. (c) The SAL (\mathcal{L}_{SAL}) serves as an auxiliary regularization term that promotes alignment between predicted emotional intensity values and ground-truth labels via a KL-based loss. These components work collaboratively to enhance multimodal representation learning.

3. Methodology

In this section, we first introduce the task definition and the overview of our MS-Mix framework. We then describe the details of each module in MS-Mix. The complete MS-Mix process is presented in Algorithm 1.

Algorithm 1: Training Procedure of MS-Mix

Input: Data \mathbf{X} and label \mathbf{Y} , backbone f_θ , prediction head f_ψ , hyperparameters α, δ, β

- 1 Initialize parameters;
- 2 **for** each epoch **do**
- 3 Sample mini-batch B ;
- 4 // Step 1: Sentiment-Aware Sample Selection Extract features $\mathbf{Z}^m = f_\theta(\mathbf{X})$ for each modality;
- 5 Compute averaged similarity across modalities;
- 6 Select consistent pairs where $s_{ij} > \delta$;
- 7 **for** each consistent pair $((x_i, y_i), (x_j, y_j))$ **do**
- 8 // Step 2: Intensity-Guided Mixing
- 9 Predict intensities I^m via \mathbf{Z}^m ;
- 10 Obtain modality specific mixing ratios $\lambda_{i,j}^m$, and mixing ratios $\lambda_{i,j}^L$ of labels;
- 11 Generate mixed features $\hat{\mathbf{z}}^m = \lambda_{i,j}^m \mathbf{z}_i^m + (1 - \lambda_{i,j}^m) \mathbf{z}_j^m$, and mixed label $\hat{y} = \lambda_{i,j}^L y_i + (1 - \lambda_{i,j}^L) y_j$;
- 12 // Step 3. Losses & Update
- 13 Task loss: $\mathcal{L}_{\text{task}} \leftarrow \text{MSE}(f_\psi(f_\theta(x)), y)$;
- 14 Mixed MSE loss: $\mathcal{L}_{\text{mixMSE}} \leftarrow \text{MSE}(f_\psi(f_\theta(\hat{\mathbf{x}})), \hat{y})$;
- 15 Alignment loss: $\mathcal{L}_{\text{SAL}} \leftarrow \text{KL}(P^L || P^m)$;
- 16 Total loss: $\mathcal{L}_{\text{total}} = \mathcal{L}_{\text{task}} + \xi_1 \cdot \mathcal{L}_{\text{mixMSE}} + \xi_2 \cdot \mathcal{L}_{\text{SAL}}$;
- 17 Update θ by minimizing $\mathcal{L}_{\text{total}}$;
- 18 **end**
- 19 **end**
- 20 **return** Trained $f_\psi \circ f_\theta$;

3.1. Task Definition and Framework Overview

Given a MSA dataset with n samples, $\mathbf{X} = (\mathbf{x}_1, \mathbf{x}_2, \dots, \mathbf{x}_n)$ and $\mathbf{Y} = (y_1, y_2, \dots, y_n)$ where y_i are continuous sentiment intensity scores, each $\mathbf{x}_i \in \mathbf{X}$ comprises data from the text (t), video (v), and audio (a) modalities, denoted as $\{\mathbf{x}_i^t, \mathbf{x}_i^v, \mathbf{x}_i^a\}$. The goal of the MSA task is to learn a mapping function $\mathcal{F} : \mathbf{X} \mapsto \mathbf{Y}$ to predict the continuous intensity of each emotion category. This mapping is realized by a backbone f_θ followed by a prediction head f_ψ .

To address data scarcity and enhance generalization in this regression-based MSA task, we propose MS-Mix. This novel latent-space data augmentation method operates on the multimodal features output by the encoder and is applied before feature fusion. As illustrated in Fig.2, the input to MS-Mix consists of multimodal features derived from the model’s encoder outputs. The SASS strategy first identifies feature pairs suitable for mixing, which are

then adaptively blended through the SIG module to generate augmented features. Both the original and synthesized features are subsequently fed into the fusion module. Additionally, the SAL serves as an auxiliary regularization term to jointly optimize the entire network and the SIG module.

As a common starting point for many mixup-based augmentation methods, vanilla mixup [13] employs a ratio λ to construct a mixed sample $(\hat{\mathbf{x}}, \hat{y})$ by performing global linear interpolation directly on the sample pair $\{(\mathbf{x}_i, y_i), (\mathbf{x}_j, y_j)\}$:

$$\begin{aligned}\hat{\mathbf{x}} &= \lambda \cdot \mathbf{x}_i + (1 - \lambda) \cdot \mathbf{x}_j, \\ \hat{y} &= \lambda \cdot y_i + (1 - \lambda) \cdot y_j,\end{aligned}\tag{1}$$

where the λ is sampled from $Beta(\alpha, \alpha)$ distribution. We define the process of Eq.1 as follows: Given the sample mixup function $H(\cdot)$, the label mixup function $G(\cdot)$, and a mixing ratio λ , we can generate the mixed sample $(\hat{\mathbf{x}}, \hat{y})$ with $\hat{\mathbf{x}} = H(\mathbf{x}_i, \mathbf{x}_j, \lambda)$, $\hat{y} = G(y_i, y_j, \lambda)$.

Mixing of original data can easily lead to sentiment semantic confusion in generated data [34]. Therefore, for each batch of data, we choose to learn different mixing ratios λ^m to mix the features $\mathbf{Z}^m = f_\theta(\mathbf{X}) \in \mathbb{R}^{B \times d^m}$ of each modal in the latent space separately (Eq. 2), and calculate the label ratio λ^L to mix the labels as follows:

$$\begin{aligned}\hat{\mathbf{z}}^m &= H(f_\theta(\mathbf{x}_i^m), f_\theta(\mathbf{x}_j^m), \lambda^m), \mathbf{x}^m \in \mathbf{X}, \\ \hat{y} &= G((y_i, y_j), \lambda^L), y \in \mathbf{Y},\end{aligned}\tag{2}$$

where $\hat{\mathbf{z}}^m$ represents the mixed features, $m \in \{t, v, a\}$ represents the set of the three modalities in the dataset, B is the mini-batch size, d^m is the hidden space dimension of modality m , and f_θ is the backbone.

Finally, the mixed and original features will be fused into a single set for subsequent feature fusion.

3.2. Sentiment-Aware Sample Selection

Emotional expressions exhibit significant variation across samples. While random in-batch mixing enhances feature smoothness, it often fails to preserve semantic consistency in the emotional space. This may lead to the mixing of two semantically opposite samples with strong emotion into a mixed sample with a neutral label and semantic confusion features. Therefore, we proposed the SASS strategy based on emotional semantic distance and screened the feature samples within each batch before mixing. Specifically, we use the cosine distance between each sample to represent semantic information similarity [38], and mix sample pairs with similarity greater than the threshold δ within each batch. This ensures that only samples with analogous emotions are combined, a critical factor that previous methods overlooked [17].

We first performed L_2 normalization on the features of each modality \mathbf{Z}^m within the batch to ensure consistent feature scaling across modalities:

$$\mathbf{Z}_{\text{norm}}^m = \frac{\mathbf{Z}^m}{\sqrt{\sum_{i=1}^{d^m} (Z_i^m)^2}}.\tag{3}$$

Then, we obtain the similarity matrix \mathbf{S} as:

$$\mathbf{S} = \sum_{m \in t, v, a} \mathbf{z}_{\text{norm}}^m \cdot (\mathbf{z}_{\text{norm}}^m)^\top / 3. \quad (4)$$

Since the matrix \mathbf{S} is symmetric ($s \in \mathbf{S}, s_{ij} = s_{ji}$) and the diagonal elements represent the self-similarity, we define the normalized upper triangular matrix \mathbf{S}' as:

$$\mathbf{S}' = \frac{1}{n(n-1)} \sum_{i \neq j} s_{ij}. \quad (5)$$

We randomly selected B pairs to mix from the feature pairs $\{(\mathbf{z}_i, y_i), (\mathbf{z}_j, y_j)\}, \mathbf{z} \in \mathbf{Z}$, with a similarity greater than $\delta = 0.2$. Our SASS strategy employs the similarity threshold to exclude sample pairs with opposite emotions before mixing. A lower threshold effectively prevents semantic confusion in the mixed samples while maximizing data diversity.

3.3. Sentiment Intensity Guided Mixing Module

The mixing ratio λ is one of the most important hyperparameters in mixup-based methods, controlling the degree of mixing between two or more samples. λ is usually sampled from the $Beta(\alpha, \alpha)$ distribution. However, in recent years, some methods [39, 30, 33] have automatically optimized mix ratios based on sample states, thereby achieving better alignment between the data and the labels.

To ensure that samples with richer emotional semantics contribute more substantially to the mixing process, we propose the SIG mixing module. Specifically, for each modality, a Multi-Head self-Attention (MHA) [40] encoder is trained to predict emotional intensity values \mathbf{I}^m . This encoder comprises an MHA layer, a residual connection, layer normalization, and a tanh activation function. The modality-specific emotional intensity predictor is denoted as f_ϕ^m (Eq. 6-8). These predictions are then used as weighting factors to adjust the mixing ratios λ^m during augmentation dynamically.

$$head_i = \text{Softmax} \left(\frac{\mathbf{z}^m \mathbf{W}_i^Q \cdot \mathbf{z}^m (\mathbf{W}_i^K)^\top}{\sqrt{d_k}} \right) \mathbf{z}^m \mathbf{W}_i^V, \quad (6)$$

$$\text{MHA}(\mathbf{Z}^m) = \text{LN}(\text{Concat}(head_1, head_2, \dots, head_h) \mathbf{W}^O + \mathbf{Z}^m), \quad (7)$$

$$\mathbf{I}^m = f_\phi^m(\mathbf{Z}^m) = \tanh(\text{GobalPool}(\text{MHA}(\mathbf{Z}^m))). \quad (8)$$

where $\mathbf{W}^{\{Q, K, V\}} = \{\mathbf{W}^Q, \mathbf{W}^K, \mathbf{W}^V\}$ are learnable weight matrices that map the input features to queries Q , keys K , and values V , d_k is the dimension of K , LN denotes Layer Normalization [41], the number of attention heads h is set to 4 or 6, and \mathbf{W}^O is the output linear transformation matrix.

Based on the intensity of emotions \mathbf{I}^m in Eq. 8, we perform Min-Max normalization on it in modality, which can further calculate the intermediate mixing weights ω_i^m for each feature pair $\{(\mathbf{z}_i, y_i), (\mathbf{z}_j, y_j)\}$:

$$\omega_i^m = \frac{|\mathbf{I}_i^m| - \min(\mathbf{I}^m)}{\max(\mathbf{I}^m) - \min(\mathbf{I}^m) + \epsilon}, \quad (9)$$

where ϵ represents the minimum value that prevents division by zero and is set to 10^{-8} . Due to the mixed strategy of convex combination, the adaptive mixing ratio $\lambda_{i,j}^m$ between the \mathbf{z}_i and \mathbf{z}_j is:

$$\lambda_{i,j}^m = \left(\frac{\omega_i^m}{\omega_i^m + \omega_j^m} + \lambda_{base} \right) / 2, \quad (10)$$

where the λ_{base} sampled from the Beta(α, α). Then, we calculate the average of the mixing ratios λ^m for each modality to obtain the mixing ratio $\lambda_{i,j}^L$ of the labels:

$$\lambda_{i,j}^L = \sum_{m \in \{t, v, a\}} \lambda_{i,j}^m / 3. \quad (11)$$

Finally, we can get the mixed feature $\hat{\mathbf{z}}^m$ and mixed label \hat{y} using Eq. 2. Unlike previous Mixup-based studies [13, 34, 15, 16], our proposed SIG module adaptively determines the mixing ratios between samples based on sentiment intensity, thereby maintaining end-to-end trainability and enabling continuous optimization throughout training.

3.4. Sentiment Alignment Loss Function

To enhance the accuracy of the emotion intensity predictor, we introduce the SAL as an additional regularization term to align the predicted distribution with the ground-truth labels. Formally, our goal is to learn a mapping from an input sample \mathbf{x} to its corresponding label y using a network $f_\psi \circ f_\theta$. The network parameters ψ and θ are typically optimized by minimizing a task-specific loss \mathcal{L}_{task} :

$$\min_{\psi, \theta} \mathcal{L}_{task}(f_\psi(f_\theta(\mathbf{x})), y). \quad (12)$$

Since the emotional labels are continuous values [42, 43, 44], we consider the mixup regression task. Therefore, we get the mapping between the mixed $\hat{\mathbf{x}}$ and \hat{y} by optimizing mixed Mean Squared Error (MSE) loss \mathcal{L}_{mixMSE} (Eq.13). By minimizing \mathcal{L}_{mixMSE} (Eq.14), the consistency between the mixed samples and labels is constrained.

$$\mathcal{L}_{mixMSE} = \lambda_{i,j}^L \cdot MSE(f_\psi(f_\theta(\hat{\mathbf{x}}_i)), y_i) + (1 - \lambda_{i,j}^L) \cdot MSE(f_\psi(f_\theta(\hat{\mathbf{x}}_j)), y_j). \quad (13)$$

$$\min_{\psi, \theta} \mathcal{L}_{mixMSE}(f_\psi(f_\theta(\hat{\mathbf{x}})), \hat{y}). \quad (14)$$

The KL divergence [45] is commonly used to measure the amount of information lost when an approximate distribution is used to represent a true distribution. A smaller KL divergence indicates that the two distributions are more similar. Thus, in this study, we introduce the SAL based on the KL divergence to align the predicted sentiment distribution with the ground-truth labels, thereby enhancing the accuracy of the emotion intensity predictor. Specifically, we convert \mathbf{I}^m and ground truth \mathbf{Y} into probability distributions \mathbf{P}^m and \mathbf{P}^L (Eq.15), then calculate the KL divergence between them (Eq.16). Finally, we scale the KL divergence and incorporate it as an additional regularization term (Eq. 17). The scale factor β is 10^3 . This approach further promotes alignment across different modalities in emotion label prediction.

$$\mathbf{P}_i^m = \frac{\exp(\mathbf{I}^m)}{\sum_{i=1}^B \exp(\mathbf{I}_i^m)}, \mathbf{P}_i^L = \frac{\exp(\mathbf{Y})}{\sum_{i=1}^B \exp(y_i)}, \quad (15)$$

$$\text{KL}(\mathbf{P}^L || \mathbf{P}^m) = \frac{1}{B} \sum_{i=1}^B \mathbf{P}_i^L (\log \mathbf{P}_i^L - \log \mathbf{P}_i^m), \quad (16)$$

$$\mathcal{L}_{SAL} = \sum_{m \in \{t, v, a\}} \text{KL}(\mathbf{P}^L || \mathbf{P}^m) \cdot \beta. \quad (17)$$

In summary, the total loss \mathcal{L}_{total} for model optimization is expressed as a joint loss defined as follows:

$$\mathcal{L}_{total} = \mathcal{L}_{task} + \xi_1 \cdot \mathcal{L}_{mixMSE} + \xi_2 \cdot \mathcal{L}_{SAL}. \quad (18)$$

where ξ_1 and ξ_2 are the weight hyperparameters used to regulate mixed MSE loss and SAL loss, respectively, with the effects to be evaluated in Section 4.6. The SAL can serve as an auxiliary regularization term that not only facilitates training of the modality-specific predictor f_ϕ^m but also promotes consistency across modalities.

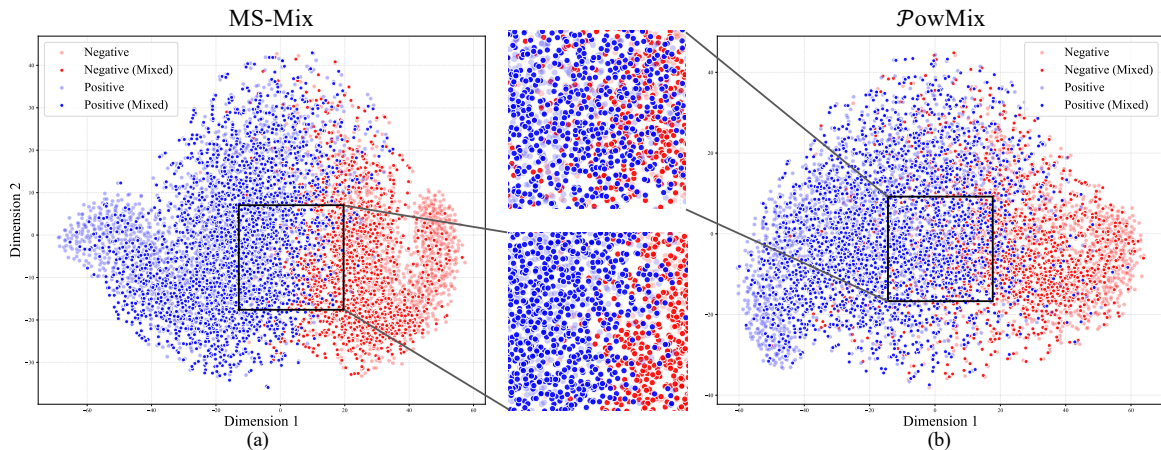


Figure 3: The t-SNE visualization of the original features and mixed features generated by MS-Mix (a) and $\mathcal{P}owMix$ (b) on the MOSEI dataset using the MISA model. We employ a color scheme (blue/red) to differentiate the positive and negative categories, and use transparency to distinguish the original features from the mixed ones.

4. Experiments

To evaluate the proposed approach, we conducted comprehensive experiments on three public MSA datasets: CMU-MOSI (MOSI) [42], CMU-MOSEI (MOSEI) [43], and CH-SIMS (SIMS) [44]. We compare our method against four representative Mixup-based methods [34, 18, 17, 33] on six state-of-the-art backbones [21, 22, 12, 46, 5, 6]. The comparative results are summarized in Tables 1,2,3. In addition, we conducted extensive ablation experiments (Table 4) and parameter sensitivity analysis (Fig. 5), as well as visualizations of the model performance (Fig. 3 and 4).

4.1. Datasets

These datasets differ in scale, data collection methods, and linguistic characteristics, thereby offering diverse and challenging testbeds for evaluating model robustness and generalization. We briefly describe the key characteristics of these datasets below:

MOSI. The MOSI [42] dataset is an English benchmark for emotion recognition, consisting of 2,199 opinion segments from 93 YouTube movie reviews. It offers aligned text (transcripts), audio, and visual (facial) data, annotated with sentiment intensity on a continuous scale from -3 (strongly negative) to +3 (strongly positive) by five independent annotators, with final labels calculated as the average of the annotators’ scores. The dataset reflects real-world complexity, including modality incongruity (e.g., sarcasm), and contains about 2.2 hours of video from 89 speakers. Widely used in multimodal fusion research, this dataset comprises pre-extracted features (e.g., acoustic data and facial action units) alongside speaker metadata.

MOSEI. The MOSEI [43] dataset includes 23,453 video segments from more than 1,000 different speakers covering over 250 topics. It is the largest multimodal benchmark for sentiment and emotion analysis. The dataset provides aligned text transcripts, audio signals, and visual frames, all annotated by trained annotators with continuous sentiment intensity scores ranging from -3 to 3 (e.g., MOSI) and six emotion intensities (happiness, sadness, anger, fear, disgust, surprise). It captures real-world communication nuances, including cross-modal conflicts, and supports research in multimodal fusion, emotion recognition, and sarcasm detection. Preprocessed features of MOSI and MOSEI are available through the CMU-Multimodal SDK [47].

SIMS. The SIMS [44] dataset is a Chinese multimodal benchmark featuring 2,281 video segments from 200 diverse online videos (vlogs, reviews, dialogues). It provides aligned text transcripts, audio, and visual data, with unified sentiment scores on a continuous scale from -1 (strongly negative) to +1 (strongly positive). As the first Chinese dataset to emphasize cross-modal dynamics, SIMS supports research on asynchronous multimodal fusion, cross-modal interaction modeling, and Mandarin sentiment analysis, with raw videos and preprocessed features publicly available.

4.2. Backbones and Baseline Methods

To enable a comprehensive and systematic evaluation, we compared the proposed method against four representative mixup-based augmentation approaches: Manifold Mixup [34] performs random mixing in the latent space to encourage smoother decision boundaries; Multi-Mix [18] is specifically designed for multimodal fusion through modality-specific mixing operations; PowMix [17] introduces a weight-aware mixing strategy that dynamically adjusts the mixing ratios according to the importance of each modality. AdvMixUp [33] leverages adversarial training to generate sample-dependent hard mixed samples using feature-level masks. We extend this method to the MSA task by adapting the input from raw images to features and applying modality-specific mixing for each modality.

These comparisons were conducted across six widely-used MSA architectures: TFN [21], LMF [22], MuIT [12], MISA [46], ALMT [5], and GLoMo [6]. These backbones encompass a broad range of feature extraction paradigms and fusion strategies, spanning from early influential works to more recent state-of-the-art approaches in MSA. All models were implemented using available code and evaluated under identical settings using the M-SENA framework [4].

4.3. Experimental Settings

Evaluation Metrics. We use the evaluation metrics defined in the M-SENA unified framework [4] to ensure consistent, comparable results. These include binary accuracy (ACC_2) and F1-score ($F1$), multiclass accuracy (ACC_5 , ACC_7) and Mean Absolute Error (MAE). Among these, MAE is a regression metric. Classification accuracy values are derived by mapping the regression scores to discrete sentiment categories. The prefix " w -" denotes the absence of neutral-labeled samples. Furthermore, to facilitate intuitive and comprehensive comparisons across metrics, we have presented the average values ($Avg.$) for all ACC and $F1$ metrics separately.

Experimental Details. The experiments utilized high-performance servers equipped with an NVIDIA GeForce RTX 3090 Ti or an NVIDIA H20 GPU. The code was implemented in Python 3.10.18 using the PyTorch 2.7.1 framework with CUDA 12.6 support. In MS-Mix, the base mixing ratio λ_{base} is sampled from a symmetric Beta distribution with $\alpha = 2.0$, and the similarity threshold δ is fixed at 0.2. The loss weights ξ_1 and ξ_2 are set to 0.7 and 0.5, respectively. Additionally, the number of attention heads h is 4 for the MOSI and MOSEI and 6 for the SIMS dataset.

4.4. Verification Performance of MS-Mix

This chapter evaluates MS-Mix on three publicly available MSA datasets: MOSI [42], MOSEI [43], and SIMS [44]. Experiments were conducted using six backbone models, representing both classical [21, 22, 12, 46] and state-of-the-art approaches [5, 6] in terms of model architectures and fusion strategies, to demonstrate the general applicability of MS-Mix across different frameworks. For each model, we compared against classical Mixup variants, including Manifold Mixup (Manifold Mix) [34] and Multimix [18], as well as a recently proposed mixup-based method in MSA, $PowMix$ [17], and the adversarial-based Mixup method, AdvMixUp [33].

To enhance the reliability and robustness of our results, all experiments were conducted five times with different random seeds, and we report the mean and standard deviation (std) for each metric. As shown in Tables 1 to 3, MS-Mix achieves top performance, ranking first or second across all metrics compared with the baseline and other mixup-based methods. It is particularly noteworthy that MS-Mix consistently outperforms all competing approaches on the comprehensive $Avg.$ metric across every backbone model.

The consistent outperformance of MS-Mix across diverse backbones and datasets stems from its core design principles, which directly address key limitations in existing mixup-based augmentation methods. Unlike these methods, which often rely on random or offline mixing strategies, MS-Mix incorporates three interconnected mechanisms tailored for MSA: First, the SASS strategy prevents the blending of semantically contradictory samples (e.g., happy and angry) by filtering pairs based on emotional similarity in the latent space. In contrast, the comparative methods [34, 18, 17, 33] mix random sample pairs regardless of emotional coherence, often yielding ambiguous or noisy samples that mislead the training process. By ensuring semantic and label consistency, SASS significantly enhances the quality of augmented data. Second, the SIG mixing module adaptively determines modality-specific mixing ratios based on emotional salience, rather than using random or fixed values as in

Table 1: Results of Various Approaches on The **MOSI** Dataset (Mean \pm std over 5 Independent Runs). **Bold**: Best performance. †: result reported in [4].

MODEL	w-ACC ₂ (%) \uparrow	ACC ₂ (%) \uparrow	w-F1(%) \uparrow	F1(%) \uparrow	ACC ₅ (%) \uparrow	ACC ₇ (%) \uparrow	MAE \downarrow	Avg.(%) \uparrow
TFN [†]	79.08	77.99	79.11	77.95	39.39	34.46	0.947	64.66
+ Manifold Mix	79.26 \pm 1.07	78.13 \pm 1.12	79.07 \pm 1.04	78.15 \pm 1.11	39.02 \pm 1.15	35.23 \pm 0.74	0.921 \pm 0.012	64.81 \pm 0.95
+ MultiMix	79.43 \pm 0.63	78.22 \pm 1.51	79.31 \pm 1.05	78.03 \pm 1.12	39.48 \pm 0.71	34.95 \pm 0.26	0.925 \pm 0.013	64.90 \pm 0.57
+ AdvMixUp	78.48 \pm 2.56	78.13 \pm 0.38	79.50 \pm 1.17	77.74 \pm 1.41	39.58 \pm 0.70	34.98 \pm 0.63	0.923 \pm 0.006	64.73 \pm 0.51
+ <i>Pow</i> Mix	79.64 \pm 1.42	78.18 \pm 0.83	79.35 \pm 0.96	77.95 \pm 0.97	40.11 \pm 1.08	36.16 \pm 0.44	0.919 \pm 0.006	65.23 \pm 0.31
+ MS-Mix (ours)	80.22 \pm 0.55	78.72 \pm 0.55	79.99 \pm 1.11	78.39 \pm 0.67	40.45 \pm 0.68	35.89 \pm 0.20	0.914 \pm 0.007	65.61 \pm 0.29
LMF [†]	79.18	77.90	79.15	77.80	38.13	33.82	0.950	64.33
+ Manifold Mix	79.23 \pm 1.12	77.85 \pm 1.28	79.34 \pm 0.94	77.95 \pm 0.68	37.84 \pm 1.22	34.17 \pm 0.32	0.943 \pm 0.009	64.40 \pm 0.21
+ MultiMix	79.92 \pm 0.81	78.19 \pm 0.24	80.29 \pm 0.89	78.58 \pm 0.46	38.51 \pm 0.49	35.80 \pm 0.65	0.925 \pm 0.006	65.21 \pm 0.31
+ AdvMixUp	79.27 \pm 1.06	77.84 \pm 0.25	79.40 \pm 0.62	78.63 \pm 0.53	38.16 \pm 0.48	34.70 \pm 0.90	0.928 \pm 0.004	64.67 \pm 0.41
+ <i>Pow</i> Mix	80.05 \pm 0.45	78.90 \pm 0.30	79.86 \pm 0.81	78.55 \pm 0.54	38.95 \pm 0.83	35.91 \pm 0.51	0.915 \pm 0.009	65.37 \pm 0.39
+ MS-Mix (ours)	82.02 \pm 0.26	79.16 \pm 0.32	82.01 \pm 0.16	79.27 \pm 0.68	41.90 \pm 0.42	36.52 \pm 0.50	0.879 \pm 0.003	66.81 \pm 0.13
MuIT [†]	80.98	79.71	80.95	79.63	42.68	36.91	0.878	66.81
+ Manifold Mix	81.01 \pm 0.58	80.38 \pm 1.26	80.04 \pm 1.95	79.34 \pm 0.28	41.14 \pm 1.67	36.66 \pm 1.37	0.864 \pm 0.019	66.43 \pm 0.83
+ MultiMix	81.49 \pm 0.72	80.20 \pm 0.67	81.62 \pm 0.48	80.19 \pm 0.91	42.76 \pm 0.87	37.37 \pm 0.69	0.856 \pm 0.004	67.27 \pm 0.47
+ AdvMixUp	81.20 \pm 0.55	79.19 \pm 0.27	81.64 \pm 0.39	79.57 \pm 0.74	42.64 \pm 0.75	36.51 \pm 0.46	0.859 \pm 0.007	66.79 \pm 0.28
+ <i>Pow</i> Mix	81.44 \pm 0.56	79.70 \pm 0.62	81.38 \pm 0.52	79.53 \pm 0.84	41.57 \pm 0.62	36.39 \pm 0.87	0.876 \pm 0.04	66.67 \pm 0.27
+ MS-Mix (ours)	82.02 \pm 0.28	79.69 \pm 0.66	81.97 \pm 0.40	79.89 \pm 0.84	43.33 \pm 0.67	37.48 \pm 0.66	0.830 \pm 0.006	67.40 \pm 0.11
MISA [†]	83.54	81.84	83.58	81.82	47.08	41.37	0.777	69.87
+ Manifold Mix	83.03 \pm 0.84	81.49 \pm 0.53	83.07 \pm 0.84	81.47 \pm 0.51	48.00 \pm 0.85	41.84 \pm 0.38	0.762 \pm 0.013	69.82 \pm 0.42
+ MultiMix	82.91 \pm 0.66	81.80 \pm 0.41	82.97 \pm 0.91	81.88 \pm 0.51	47.40 \pm 0.77	42.04 \pm 0.36	0.751 \pm 0.005	69.83 \pm 0.31
+ AdvMixUp	83.44 \pm 0.47	81.39 \pm 0.50	83.34 \pm 0.50	81.34 \pm 0.69	47.59 \pm 0.59	41.56 \pm 0.65	0.762 \pm 0.007	69.78 \pm 0.26
+ <i>Pow</i> Mix	83.17 \pm 0.80	81.45 \pm 0.65	83.43 \pm 0.46	81.41 \pm 0.47	48.16 \pm 0.31	42.03 \pm 0.55	0.757 \pm 0.010	69.94 \pm 0.36
+ MS-Mix (ours)	83.94 \pm 0.52	82.21 \pm 0.63	83.81 \pm 0.32	82.14 \pm 0.37	48.59 \pm 0.56	42.36 \pm 0.31	0.746 \pm 0.005	70.51 \pm 0.19
ALMT	83.48 \pm 0.80	82.06 \pm 0.61	83.39 \pm 0.78	81.94 \pm 0.59	51.32 \pm 0.75	45.46 \pm 0.86	0.733 \pm 0.003	71.28 \pm 0.23
+ Manifold Mix	84.16 \pm 0.76	82.58 \pm 0.82	83.58 \pm 0.50	82.60 \pm 0.77	51.51 \pm 0.93	46.04 \pm 1.39	0.734 \pm 0.008	71.74 \pm 0.15
+ MultiMix	83.53 \pm 0.71	82.05 \pm 0.38	83.31 \pm 1.03	81.89 \pm 0.61	48.92 \pm 0.74	44.21 \pm 0.65	0.747 \pm 0.005	70.65 \pm 0.38
+ AdvMixUp	83.95 \pm 0.23	81.94 \pm 0.35	83.61 \pm 0.67	81.95 \pm 0.68	51.44 \pm 1.20	46.89 \pm 0.59	0.726 \pm 0.004	71.63 \pm 0.21
+ <i>Pow</i> Mix	83.38 \pm 0.50	82.34 \pm 0.96	83.26 \pm 0.84	82.33 \pm 0.93	51.67 \pm 0.53	45.72 \pm 0.64	0.730 \pm 0.007	71.45 \pm 0.25
+ MS-Mix (ours)	84.02 \pm 0.51	83.21 \pm 0.60	83.93 \pm 0.33	83.02 \pm 0.28	52.33 \pm 0.65	46.98 \pm 0.37	0.721 \pm 0.004	72.25 \pm 0.32
GLoMo	83.81 \pm 0.27	82.19 \pm 0.32	83.73 \pm 0.28	82.13 \pm 0.33	52.59 \pm 0.71	47.10 \pm 0.94	0.743 \pm 0.010	71.92 \pm 0.22
+ Manifold Mix	84.78 \pm 0.43	82.95 \pm 0.62	84.80 \pm 0.23	83.00 \pm 0.70	52.89 \pm 0.96	49.45 \pm 0.99	0.731 \pm 0.006	72.98 \pm 0.18
+ MultiMix	84.94 \pm 0.56	83.23 \pm 0.58	85.02 \pm 0.49	83.32 \pm 0.58	53.01 \pm 0.47	50.46 \pm 0.93	0.728 \pm 0.004	73.33 \pm 0.22
+ AdvMixUp	84.27 \pm 0.73	83.24 \pm 0.65	84.39 \pm 0.59	83.25 \pm 0.65	53.27 \pm 0.49	51.09 \pm 0.68	0.730 \pm 0.004	73.25 \pm 0.36
+ <i>Pow</i> Mix	84.81 \pm 0.29	83.36 \pm 0.19	84.84 \pm 0.36	83.48 \pm 0.35	53.14 \pm 0.75	49.56 \pm 2.06	0.730 \pm 0.007	73.20 \pm 0.31
+ MS-Mix (ours)	85.21 \pm 0.63	83.46 \pm 0.19	85.23 \pm 0.56	83.43 \pm 0.32	54.64 \pm 0.96	52.31 \pm 0.59	0.726 \pm 0.005	74.04 \pm 0.47

Manifold Mix [34], MultiMix [18], or leveraging modality importance without emotional context like *Pow*Mix [17] and AdvMixUp [33]. This allows MS-Mix to dynamically weight each modality’s contribution, leading to more discriminative mixed features and improved robustness of learned cross-modal representations. Third, the SAL serves as a regularization term that aligns predicted sentiment distributions with ground-truth labels, enhancing prediction consistency across modalities and providing additional supervisory signal. This component is unique to MS-Mix and offers a critical advantage over comparative methods, which lack explicit constraints on the alignment of emotion-level distributions. As a result, SAL not only stabilizes training but also strengthens the model’s resistance to overfitting.

4.5. Performance Visualization

To further demonstrate the effectiveness of MS-Mix, we conduct both t-SNE [48] visualizations (Fig. 3) and loss landscape visualizations (Fig. 4). Specifically, we employ t-SNE to project the distributions of textual features for both the original and mixed features extracted from the MOSEI dataset, using the MISA model. The results reveal that features generated by MS-Mix exhibit significantly clearer decision boundaries and more distinct cluster separa-

Table 2: Results of Various Approaches on the **MOSEI** Dataset (Mean \pm std over 5 Independent Runs). **Bold**: Best performance. †: result reported in [4].

MODEL	w-ACC ₂ (%) \uparrow	ACC ₂ (%) \uparrow	w-F1(%) \uparrow	F1(%) \uparrow	ACC ₅ (%) \uparrow	ACC ₇ (%) \uparrow	MAE \downarrow	Avg.(%) \uparrow
TFN [†]	81.89	78.50	81.74	78.96	53.10	51.60	0.573	70.97
+ Manifold Mix	83.41 \pm 0.73	81.42 \pm 0.48	83.42 \pm 0.61	81.51 \pm 0.65	52.87 \pm 0.65	51.25 \pm 0.72	0.571 \pm 0.003	72.31 \pm 0.19
+ MultiMix	82.73 \pm 0.50	80.61 \pm 0.63	82.46 \pm 0.64	80.46 \pm 0.98	53.17 \pm 0.74	51.74 \pm 0.64	0.569 \pm 0.003	71.86 \pm 0.32
+ AdvMixUp	82.85 \pm 0.51	80.77 \pm 0.71	82.96 \pm 0.65	80.98 \pm 0.54	53.32 \pm 0.63	52.20 \pm 0.69	0.566 \pm 0.002	72.18 \pm 0.16
+ <i>Pow</i> Mix	83.36 \pm 1.00	81.25 \pm 0.65	83.37 \pm 0.72	81.51 \pm 0.53	53.08 \pm 0.58	51.64 \pm 0.55	0.564 \pm 0.004	72.37 \pm 0.56
+ MS-Mix (ours)	83.41 \pm 0.39	82.16 \pm 0.26	83.30 \pm 0.49	82.07 \pm 0.31	53.87 \pm 0.44	52.20 \pm 0.29	0.559 \pm 0.002	72.84 \pm 0.17
LMF [†]	83.48	80.54	83.36	80.94	52.99	51.59	0.576	72.15
+ Manifold Mix	83.21 \pm 0.64	78.91 \pm 1.49	83.39 \pm 0.68	79.01 \pm 1.46	53.40 \pm 0.83	52.04 \pm 0.76	0.572 \pm 0.008	71.66 \pm 0.44
+ MultiMix	84.17 \pm 0.71	80.73 \pm 0.80	84.29 \pm 0.58	80.80 \pm 0.83	53.72 \pm 0.88	52.72 \pm 0.96	0.564 \pm 0.002	72.74 \pm 0.36
+ AdvMixUp	84.12 \pm 0.55	81.72 \pm 0.81	84.12 \pm 0.63	81.79 \pm 0.75	53.47 \pm 1.04	52.14 \pm 0.77	0.565 \pm 0.008	72.90 \pm 0.38
+ <i>Pow</i> Mix	83.95 \pm 0.31	80.97 \pm 0.59	84.02 \pm 0.30	81.27 \pm 0.53	54.37 \pm 0.59	52.73 \pm 0.74	0.560 \pm 0.006	72.88 \pm 0.30
+ MS-Mix (ours)	84.53 \pm 0.54	82.99 \pm 0.48	84.60 \pm 0.40	83.04 \pm 0.38	54.45 \pm 0.43	52.65 \pm 0.47	0.556 \pm 0.004	73.71 \pm 0.27
MuIT [†]	84.63	81.15	84.52	81.56	54.51	52.84	0.559	73.20
+ Manifold Mix	84.39 \pm 0.27	81.31 \pm 1.19	84.32 \pm 0.25	81.55 \pm 1.01	53.94 \pm 0.48	52.39 \pm 0.48	0.562 \pm 0.002	72.98 \pm 0.58
+ MultiMix	83.99 \pm 0.36	81.45 \pm 0.68	84.03 \pm 0.53	81.75 \pm 0.61	54.22 \pm 0.52	52.46 \pm 0.49	0.565 \pm 0.006	72.98 \pm 0.19
+ AdvMixUp	84.31 \pm 0.50	81.17 \pm 0.17	84.29 \pm 0.71	80.94 \pm 0.74	54.30 \pm 0.44	51.98 \pm 0.17	0.570 \pm 0.003	72.83 \pm 0.33
+ <i>Pow</i> Mix	84.71 \pm 0.62	81.74 \pm 0.75	84.65 \pm 0.90	81.85 \pm 0.55	54.37 \pm 0.51	52.68 \pm 0.47	0.559 \pm 0.003	73.33 \pm 0.23
+ MS-Mix (ours)	84.98 \pm 0.34	82.08 \pm 0.37	84.87 \pm 0.73	82.19 \pm 0.33	55.00 \pm 0.39	53.04 \pm 0.28	0.555 \pm 0.003	73.69 \pm 0.27
MISA [†]	84.67	80.67	84.66	81.12	53.63	52.05	0.558	72.80
+ Manifold Mix	84.51 \pm 0.81	80.24 \pm 2.22	84.57 \pm 0.73	81.18 \pm 1.99	54.49 \pm 0.55	52.83 \pm 0.69	0.548 \pm 0.006	72.90 \pm 0.90
+ MultiMix	84.23 \pm 0.53	81.31 \pm 0.47	84.20 \pm 0.68	81.26 \pm 0.33	54.07 \pm 0.47	52.66 \pm 0.38	0.552 \pm 0.002	72.95 \pm 0.33
+ AdvMixUp	84.65 \pm 0.58	81.69 \pm 0.49	84.55 \pm 0.93	81.64 \pm 0.64	54.79 \pm 0.57	52.69 \pm 0.35	0.544 \pm 0.009	73.34 \pm 0.19
+ <i>Pow</i> Mix	84.49 \pm 0.49	82.03 \pm 0.29	84.19 \pm 0.38	81.95 \pm 0.19	54.79 \pm 0.46	52.20 \pm 0.62	0.547 \pm 0.003	73.27 \pm 0.18
+ MS-Mix (ours)	84.84 \pm 0.31	83.15 \pm 0.36	84.72 \pm 0.33	83.08 \pm 0.51	55.04 \pm 0.34	52.95 \pm 0.43	0.542 \pm 0.004	73.96 \pm 0.28
ALMT	85.15 \pm 0.80	81.35 \pm 0.56	85.04 \pm 0.48	81.53 \pm 0.50	54.11 \pm 0.29	52.73 \pm 0.32	0.550 \pm 0.003	73.32 \pm 0.14
+ Manifold Mix	85.13 \pm 1.46	82.16 \pm 1.06	85.08 \pm 1.33	81.65 \pm 2.73	54.33 \pm 0.83	52.65 \pm 1.00	0.543 \pm 0.005	73.33 \pm 1.19
+ MultiMix	85.10 \pm 1.02	82.00 \pm 0.73	85.22 \pm 0.60	81.96 \pm 0.78	54.70 \pm 0.74	52.70 \pm 0.70	0.538 \pm 0.007	73.61 \pm 0.50
+ AdvMixUp	85.22 \pm 0.56	81.99 \pm 0.32	85.05 \pm 0.64	82.03 \pm 0.42	54.46 \pm 0.54	52.87 \pm 0.30	0.544 \pm 0.008	73.60 \pm 0.32
+ <i>Pow</i> Mix	85.55 \pm 0.46	82.37 \pm 0.45	85.48 \pm 0.51	82.35 \pm 0.26	54.58 \pm 0.69	53.13 \pm 0.45	0.539 \pm 0.004	73.91 \pm 0.23
+ MS-Mix (ours)	85.41 \pm 0.62	82.90 \pm 0.66	85.62 \pm 0.55	83.08 \pm 0.56	55.17 \pm 0.21	53.55 \pm 0.36	0.536 \pm 0.003	74.29 \pm 0.30
GLoMo	84.93 \pm 0.80	82.71 \pm 0.56	85.28 \pm 0.50	82.95 \pm 0.77	53.80 \pm 0.48	52.67 \pm 0.60	0.542 \pm 0.004	73.72 \pm 0.52
+ Manifold Mix	84.88 \pm 0.90	83.65 \pm 0.57	85.13 \pm 0.72	83.28 \pm 0.50	56.08 \pm 0.84	53.37 \pm 1.53	0.535 \pm 0.011	74.40 \pm 0.48
+ MultiMix	85.13 \pm 0.39	83.29 \pm 0.67	85.25 \pm 0.39	82.92 \pm 0.81	55.05 \pm 0.28	52.93 \pm 0.33	0.535 \pm 0.005	74.09 \pm 0.27
+ AdvMixUp	85.24 \pm 0.40	83.20 \pm 0.39	84.92 \pm 0.42	82.98 \pm 0.35	55.00 \pm 0.39	53.04 \pm 0.36	0.537 \pm 0.004	74.06 \pm 0.22
+ <i>Pow</i> Mix	85.08 \pm 0.20	83.19 \pm 0.23	85.12 \pm 0.26	83.38 \pm 0.48	55.08 \pm 0.29	53.07 \pm 0.27	0.533 \pm 0.003	74.15 \pm 0.07
+ MS-Mix (ours)	85.32 \pm 0.26	84.12 \pm 0.31	85.25 \pm 0.35	84.17 \pm 0.38	55.84 \pm 0.22	53.15 \pm 0.30	0.531 \pm 0.003	74.64 \pm 0.10

ration than those produced by *Pow*Mix. This enhanced separation indicates that MS-Mix not only preserves the semantic integrity of the original feature space but also yields more discriminative intermediate representations.

Furthermore, we analyze the loss landscape to examine the generalization effect of MS-Mix. The generalization ability of neural networks is closely related to the geometry of their loss landscapes, where convergence to flat minima is generally associated with superior robustness and generalization performance [49]. To visualize this, we plot the 2D loss surface of the ALMT model on MOSEI by perturbing the parameters along two random, mutually orthogonal directions, generated via Gaussian sampling and Gram-Schmidt orthogonalization. As shown in Fig. 4, introducing Manifold Mix and other variants resulted in some landscape smoothing. However, pronounced peaks and high local curvature remained, indicating persistent sensitivity to parameter perturbations. In contrast, MS-Mix yields a notably smoother, flatter landscape, suggesting reduced gradient conflict during training and convergence toward more robust minima.

In summary, by integrating the evidence from label distribution on MOSEI (Fig. 1), feature visualization (Fig. 3), and loss landscapes (Fig. 4), MS-Mix effectively mitigates the

Table 3: Results of Various Approaches on The SIMS Dataset (Mean \pm std over 5 Independent Runs). **Bold:** Best performance. †: result reported in [4].

MODEL	ACC ₂ (%) \uparrow	ACC ₃ (%) \uparrow	ACC ₅ (%) \uparrow	F1(%) \uparrow	MAE \downarrow	Avg.(%) \uparrow
TFN [†]	78.38	65.12	39.30	78.62	0.432	65.36
+ Manifold Mix	78.56 \pm 1.13	66.77 \pm 0.91	39.54 \pm 0.73	78.62 \pm 1.01	0.437 \pm 0.006	65.87 \pm 0.72
+ MultiMix	79.61 \pm 0.62	65.95 \pm 0.80	37.23 \pm 0.86	79.71 \pm 0.74	0.438 \pm 0.003	65.63 \pm 0.26
+ AdvMixUp	79.42 \pm 0.96	67.15 \pm 1.48	39.33 \pm 0.35	79.43 \pm 0.62	0.427 \pm 0.007	66.33 \pm 0.73
+ PowMix	79.85 \pm 0.56	67.89 \pm 0.67	39.50 \pm 0.44	79.95 \pm 0.52	0.428 \pm 0.003	66.80 \pm 0.29
+ MS-Mix (ours)	80.66\pm0.47	68.39\pm0.72	40.74\pm0.52	80.71\pm0.73	0.423\pm0.005	67.62\pm0.39
LMF [†]	77.77	64.68	40.53	77.88	0.441	65.22
+ Manifold Mix	78.08 \pm 0.82	65.85 \pm 0.68	38.48 \pm 0.92	78.04 \pm 0.49	0.447 \pm 0.004	65.11 \pm 0.52
+ MultiMix	77.97 \pm 0.27	65.55 \pm 0.64	37.61 \pm 1.04	77.70 \pm 0.51	0.448 \pm 0.011	64.71 \pm 0.30
+ AdvMixUp	78.09 \pm 0.71	65.96\pm0.47	39.49 \pm 0.89	78.16 \pm 0.68	0.435 \pm 0.007	65.43 \pm 0.63
+ PowMix	77.91 \pm 0.41	65.88 \pm 0.17	39.64 \pm 0.49	78.04 \pm 0.42	0.437 \pm 0.002	65.37 \pm 0.25
+ MS-Mix (ours)	78.12\pm0.24	65.80 \pm 0.30	41.02\pm0.82	78.16\pm0.37	0.433\pm0.003	65.77\pm0.20
MuIT [†]	77.46	65.43	34.79	77.57	0.446	63.81
+ Manifold Mix	78.34 \pm 0.44	64.33 \pm 0.95	34.94 \pm 2.44	78.00 \pm 0.78	0.448 \pm 0.001	63.90 \pm 0.58
+ MultiMix	77.70 \pm 1.05	64.80 \pm 0.63	36.55 \pm 0.99	77.70 \pm 0.73	0.447 \pm 0.005	64.19 \pm 0.27
+ AdvMixUp	78.10 \pm 0.54	64.27 \pm 0.71	37.61 \pm 0.51	78.20 \pm 0.47	0.445 \pm 0.006	64.55 \pm 0.50
+ PowMix	78.29 \pm 1.03	65.07 \pm 0.40	37.74 \pm 0.32	78.11 \pm 1.06	0.443 \pm 0.007	64.80 \pm 0.42
+ MS-Mix (ours)	78.51\pm0.71	65.53\pm0.43	38.16\pm0.18	78.70\pm1.13	0.443\pm0.003	65.22\pm0.48
MISA	76.53 \pm 0.82	62.96 \pm 0.29	36.01 \pm 0.64	76.71 \pm 0.90	0.452 \pm 0.004	63.05 \pm 0.44
+ Manifold Mix	76.87 \pm 0.69	63.96 \pm 0.35	37.67 \pm 0.81	77.08 \pm 0.69	0.458 \pm 0.005	63.89 \pm 0.28
+ MultiMix	77.34 \pm 0.36	64.26 \pm 0.05	37.30 \pm 1.18	77.07 \pm 1.32	0.439 \pm 0.009	63.99 \pm 0.21
+ AdvMixUp	77.01 \pm 0.80	63.82 \pm 0.48	36.47 \pm 1.02	77.22 \pm 0.52	0.450 \pm 0.010	63.63 \pm 0.40
+ PowMix	77.56 \pm 0.39	64.32 \pm 0.39	37.21 \pm 0.30	77.48 \pm 0.33	0.441 \pm 0.003	64.14 \pm 0.27
+ MS-Mix (ours)	78.19\pm0.28	64.70\pm0.59	37.75\pm0.21	78.14\pm0.44	0.434\pm0.004	64.69\pm0.23
ALMT	77.19 \pm 0.88	64.25 \pm 0.80	38.68\pm0.50	76.81 \pm 0.86	0.442 \pm 0.009	64.23 \pm 0.48
+ Manifold Mix	76.88 \pm 1.49	63.67 \pm 1.00	38.49 \pm 1.94	77.08 \pm 1.22	0.429 \pm 0.004	64.03 \pm 0.49
+ MultiMix	77.52 \pm 1.30	63.04 \pm 0.42	38.62 \pm 0.52	78.11 \pm 0.09	0.436 \pm 0.007	64.32 \pm 0.17
+ AdvMixUp	77.84 \pm 1.14	64.50 \pm 1.30	37.94 \pm 0.30	77.88 \pm 0.64	0.427 \pm 0.003	64.54 \pm 0.08
+ PowMix	77.61 \pm 0.25	64.84\pm0.77	38.44 \pm 0.61	77.87 \pm 0.34	0.424\pm0.004	64.69 \pm 0.36
+ MS-Mix (ours)	78.21\pm0.14	64.52 \pm 0.53	38.63 \pm 0.41	78.30\pm0.40	0.426 \pm 0.003	64.92\pm0.36
GLoMo	78.80 \pm 0.66	65.66 \pm 0.76	37.11 \pm 0.86	78.81 \pm 0.51	0.427 \pm 0.005	65.09 \pm 0.51
+ Manifold Mix	78.98 \pm 1.16	65.93 \pm 0.62	37.78 \pm 0.52	78.94 \pm 0.67	0.426 \pm 0.005	65.41 \pm 0.47
+ MultiMix	78.64 \pm 0.66	66.42 \pm 0.42	38.28 \pm 0.41	79.05 \pm 0.88	0.428 \pm 0.010	65.60 \pm 0.28
+ AdvMixUp	78.31 \pm 0.88	66.98 \pm 0.83	38.30 \pm 0.20	77.23 \pm 0.36	0.432 \pm 0.002	65.20 \pm 0.44
+ PowMix	79.34\pm0.65	65.11 \pm 1.94	38.33 \pm 0.42	79.12 \pm 0.18	0.428 \pm 0.007	65.47 \pm 0.45
+ MS-Mix (ours)	79.33 \pm 0.45	67.38\pm0.98	38.36\pm0.31	79.23\pm0.30	0.423\pm0.001	66.07\pm0.39

Table 4: Results of the ablation experiments using the LMF method on the MOSI database.

Bold: Best performance.

Manifold Mix	SASS	SIG	SAL	w-ACC ₂ (%) \uparrow	ACC ₂ (%) \uparrow	w-F1(%) \uparrow	F1(%) \uparrow	ACC ₅ (%) \uparrow	ACC ₇ (%) \uparrow	MAE \downarrow	Avg.(%) \uparrow
✓				79.23	77.85	79.34	77.95	37.84	34.17	0.943	64.40
✓	✓			79.98	78.41	80.08	78.60	38.86	35.26	0.921	65.20
✓		✓		80.94	78.91	80.93	79.00	40.48	35.25	0.925	65.92
✓		✓	✓	81.48	79.71	81.58	79.38	41.54	35.37	0.949	66.51
✓	✓	✓		81.41	78.03	81.41	79.61	40.48	36.00	0.919	66.16
✓	✓	✓	✓	82.02	79.16	82.01	79.27	41.90	36.52	0.879	66.81
SIG \rightarrow Ground-Truth				79.76	78.29	79.82	78.31	38.27	34.87	0.936	64.89
SIG \rightarrow Linear Mapping				80.50	78.23	80.79	78.37	39.04	34.70	0.927	65.27

semantic confusion and label mismatch issues inherent in other mixup variants. Our approach generates discriminative features with well-matched labels, thereby significantly enhancing the quality of mixed samples and improving overall performance in MSA.

4.6. Ablation and Hyperparameter Analysis

To evaluate the impact of key hyperparameters and individual algorithmic components of MS-Mix, we performed ablation studies on three core components using the LMF [22] model on the MOSI [42] and SIMS [44] datasets. Additionally, hyperparameter sensitivity analyses on the MOSEI dataset [43] were conducted using the MISA [46] and GLoMo [6] models. All

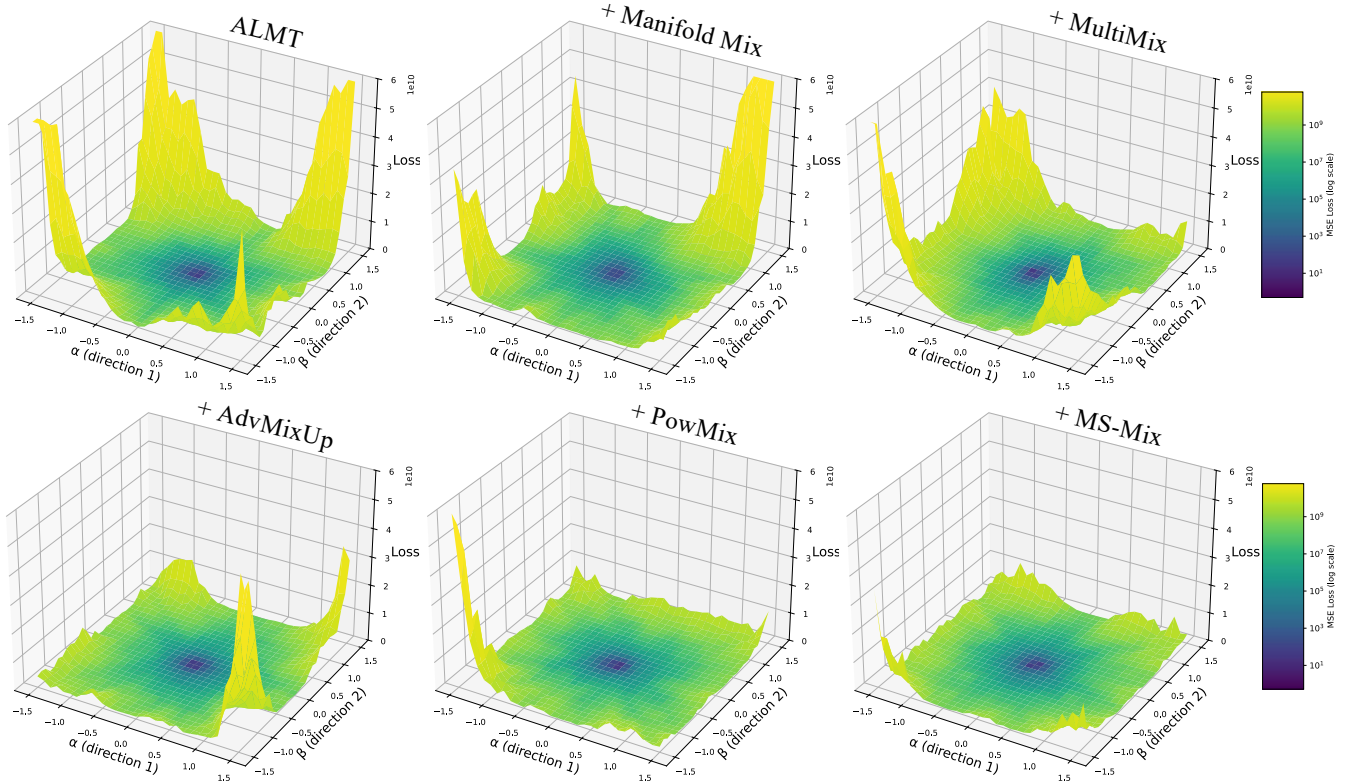


Figure 4: Visualization of loss landscapes comparing Mixup variants and MS-Mix on MOSEI using ALMT.

experiments were run five times using different random seeds, and the average values were reported as the results.

In our ablation study, we integrated Manifold Mix [34] into the classic LMF [22] backbone as the baseline to evaluate the contribution of each proposed component: SASS, SIG, and SAL. To isolate the effect of each module, we conducted experiments by selectively enabling or disabling individual components during training. Note that SAL relies on SIG’s output and thus cannot be evaluated independently. Furthermore, to justify the rationality of SIG’s complex design, we additionally investigated two simplified variants: degenerating SIG to a linear layer (SIG \rightarrow Linear Mapping) and using the absolute values of the ground-truth labels as the intensity scores directly (SIG \rightarrow Ground-Truth). All results were obtained by averaging over five independent runs with different random seeds.

As shown in the table 4, each of the three core components contributes substantially to the overall performance gains over the baseline. Removing any single module results in noticeable degradation, underscoring its individual importance. Furthermore, simplified variants of SIG also lead to clear performance drops. This is because a simple linear mapping is insufficient for extracting the complex, non-linear nature of emotional intensity, and the direct use of a global label overlooks the differences in emotional expression across modalities. In contrast, the attention-based prediction mechanism in our full SIG module effectively captures these latent, modality-specific intensity signals.

To comprehensively analyze the sensitivity of key hyperparameters, we conducted extensive experiments using both the top-performing GLoMo model [6] and the classical MISA

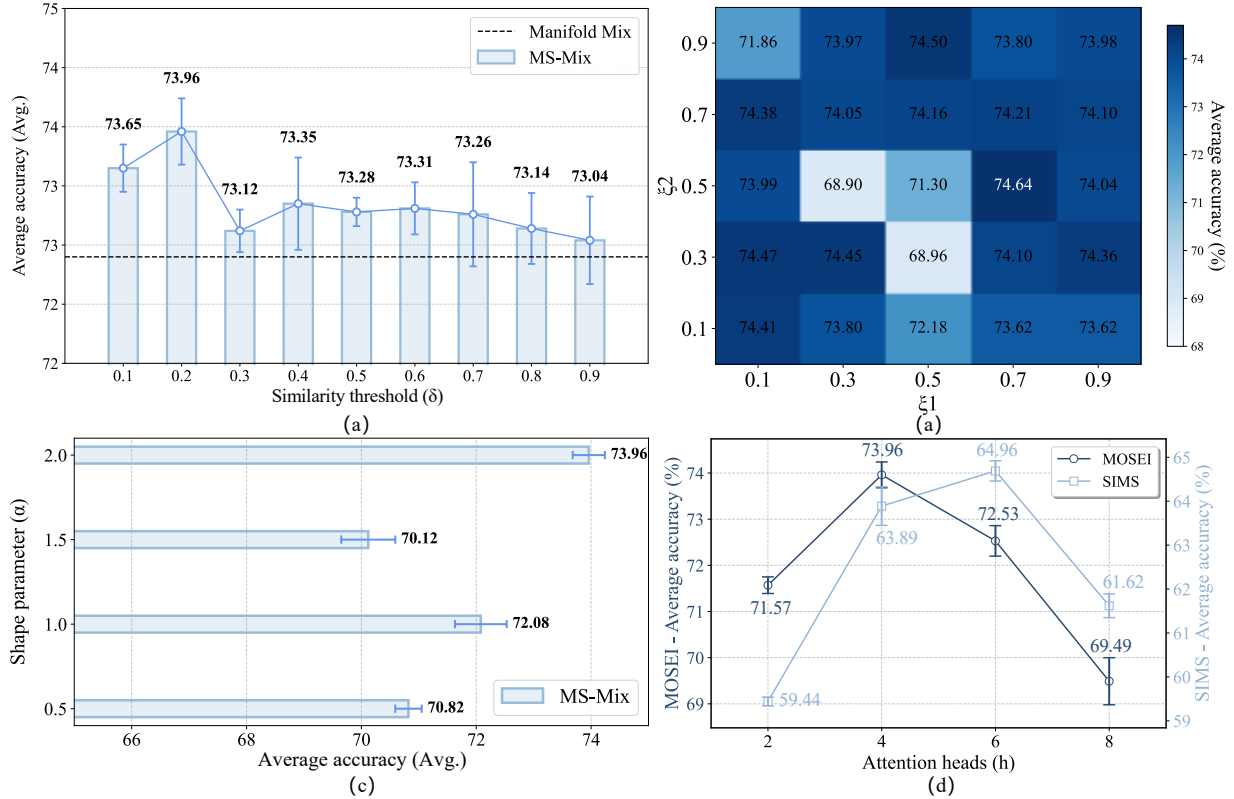


Figure 5: The impact of different parameter values. (a) Accuracy under different similarity thresholds δ . (b) Accuracy under different combinations of ξ_1 and ξ_2 . (c) Accuracy under different α . (d) Accuracy under different attention heads h .

architecture [46] on the largest English dataset MOSEI [43] and the Chinese benchmark SIMS [44]. As illustrated in Fig. 5, our evaluation shows that hyperparameters are critical to model performance. Using the MISA model on MOSEI, we first examined the similarity selection threshold δ (Fig. 5(a)). The results demonstrate that at $\delta = 0.2$, the method maintains an optimal balance, incorporating sufficient samples while effectively filtering out emotionally contradictory ones, thus achieving peak performance. Notably, even under suboptimal δ configurations, MS-Mix consistently surpasses Manifold Mix [34]. We further evaluated the loss weights ξ_1 and ξ_2 with the GLoMo model on MOSEI (Fig. 5(b)). The experimental outcomes confirm the rationality of our weight selection, showing that $\xi_1 = 0.7$ and $\xi_2 = 0.5$ yield the best performance. Additionally, we assessed the shape parameter α of the Beta distribution using MISA on MOSEI (Fig. 5(c)), finding $\alpha = 2.0$ to be optimal. The influence of the number of attention heads h was also investigated across datasets (Fig. 5(d)): $h = 4$ delivers the best results on MOSEI, while $h = 6$ is most effective on SIMS. These findings collectively validate the rationale behind our parameter configurations.

4.7. Occlusion Experiment

In the random occlusion experiment, we compared the performance of MS-Mix against baseline methods [34, 18, 17] under both clean and noisy data conditions across MOSI [42], MOSEI [43], and SIMS [44]. Specifically, we randomly masked out 0% to 40% of the input data during training of the LMF [22] model to investigate the effect of mixup-based

augmentation on model robustness.

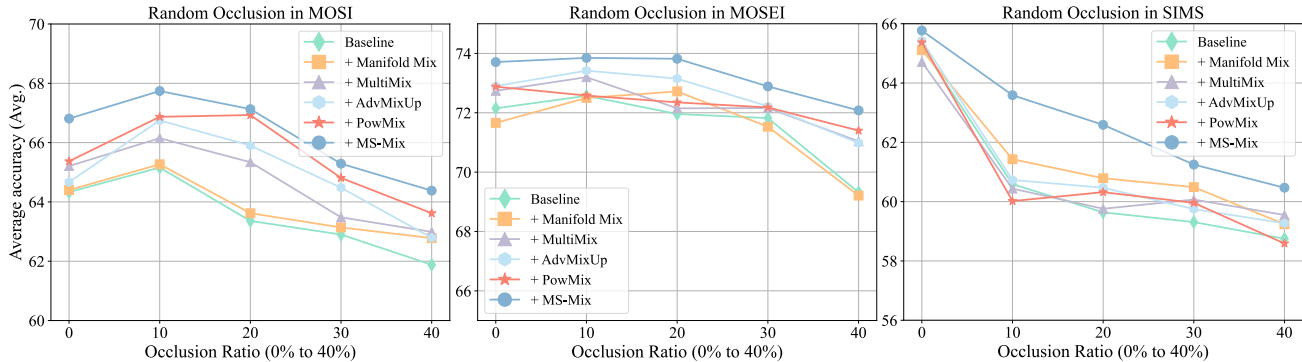


Figure 6: The performance of different mixup-based methods at different occlusion ratios on three datasets.

As shown in Fig. 6, the experimental results indicate that introducing noise affects performance across all datasets. A noteworthy phenomenon emerges: moderate levels of random masking (e.g., 10% or 20%) unexpectedly improve performance rather than degrade it. Beyond these optimal masking ratios, however, model performance deteriorates. Despite these variations, MS-Mix consistently achieves the highest average accuracy across all evaluated conditions, demonstrating its advantage in optimizing the model to handle noisy data.

5. CONCLUSION

In this paper, we propose MS-Mix, a novel, adaptive data augmentation framework designed specifically for MSA. Unlike traditional mixup-based methods, which often rely on random and offline mixing strategies, MS-Mix introduces three key emotion-aware mechanisms to enhance the semantic consistency of augmented samples. First, the SASS module ensures that only emotionally consistent samples are combined, effectively avoiding the mixing of feature pairs with contradictory emotions. Second, the SIG mixing module adaptively determines mixing ratios for each modality based on emotional salience, thereby promoting samples with clearer decision boundaries. Third, the SAL aligns the predicted emotion distributions with ground-truth labels via KL-divergence minimization, serving as an effective regularizer that improves generalization. An empirical evaluation across three benchmark datasets and six diverse backbone architectures shows that MS-Mix achieves state-of-the-art performance.

From an engineering perspective, MS-Mix enables more reliable and data-efficient multimodal emotion understanding, facilitating practical deployment in human-computer interaction, intelligent human-robot systems, and emotion-aware assistive technologies. In future work, we will consider extending MS-Mix to other multimodal tasks, such as mental health monitoring and human-computer interaction, leveraging its ability to maintain semantic consistency in a wider range of applications. Furthermore, we also intend to integrate self-supervised or semi-supervised learning strategies into MS-Mix to reduce reliance on large annotated datasets.

6. Conflicts of Interest Statement

The authors declare no conflicts of interest.

References

- [1] S. Deori, T. Chutia, H. J. Saikia, A. Boro, N. Baruah, Bridging techniques and applications in sentiment analysis: Approaches, challenges, and emerging trends, *Engineering Applications of Artificial Intelligence* 164 (2026) 113255.
- [2] Z. Li, Y. Fan, B. Jiang, T. Lei, W. Liu, A survey on sentiment analysis and opinion mining for social multimedia, *Multimedia Tools and Applications* 78 (6) (2019) 6939–6967.
- [3] X. Liu, G. He, S. Li, F. Yang, S. He, L. Chen, Multi-level feature decomposition and fusion model for video-based multimodal emotion recognition, *Engineering Applications of Artificial Intelligence* 152 (2025) 110744.
- [4] H. Mao, Z. Yuan, H. Xu, W. Yu, Y. Liu, K. Gao, M-sena: An integrated platform for multimodal sentiment analysis, in: *Proceedings of the 60th Annual Meeting of the Association for Computational Linguistics: System Demonstrations, 2022*, pp. 204–213.
- [5] H. Zhang, Y. Wang, G. Yin, K. Liu, Y. Liu, T. Yu, Learning language-guided adaptive hyper-modality representation for multimodal sentiment analysis, in: *The Conference on Empirical Methods in Natural Language Processing (EMNLP), 2023*.
- [6] Y. Zhuang, Y. Zhang, Z. Hu, X. Zhang, J. Deng, F. Ren, Glomo: Global-local modal fusion for multimodal sentiment analysis, in: *Proceedings of the 32nd ACM International Conference on Multimedia (ACM MM), 2024*, pp. 1800–1809.
- [7] L. Xiao, R. Mao, S. Zhao, Q. Lin, Y. Jia, L. He, E. Cambria, Exploring cognitive and aesthetic causality for multimodal aspect-based sentiment analysis, *IEEE Transactions on Affective Computing* (2025) 1–18.
- [8] A. Wulamu, Y. Wu, X. Liu, Y. Zhang, J. Xu, Y. Zhang, Enhanced multi-modal emotion recognition using the feature level fusion, *Engineering Applications of Artificial Intelligence* 162 (2025) 112447.
- [9] J. A. Aquino, D. J. Liew, Y.-C. Chang, Graph-aware pre-trained language model for political sentiment analysis in filipino social media, *Engineering Applications of Artificial Intelligence* 146 (2025) 110317.
- [10] T. Zhang, K. Yang, S. Ji, S. Ananiadou, Emotion fusion for mental illness detection from social media: A survey, *Information Fusion* 92 (2023) 231–246.
- [11] U. Singh, K. Abhishek, H. K. Azad, A survey of cutting-edge multimodal sentiment analysis, *ACM Computing Surveys* 56 (9) (2024) 1–38.

- [12] Y.-H. H. Tsai, S. Bai, P. P. Liang, J. Z. Kolter, L.-P. Morency, R. Salakhutdinov, Multimodal transformer for unaligned multimodal language sequences, in: Proceedings of the Association for Computational Linguistics (ACL)., Vol. 2019, 2019, p. 6558.
- [13] H. Zhang, M. Cisse, Y. N. Dauphin, D. Lopez-Paz, mixup: Beyond empirical risk minimization, in: International Conference on Learning Representations (ICLR), OpenReview.net, 2018.
- [14] N. Srivastava, G. Hinton, A. Krizhevsky, I. Sutskever, R. Salakhutdinov, Dropout: a simple way to prevent neural networks from overfitting, The journal of machine learning research (2014) 1929–1958.
- [15] S. Yun, D. Han, S. J. Oh, S. Chun, J. Choe, Y. Yoo, Cutmix: Regularization strategy to train strong classifiers with localizable features, in: Proceedings of the IEEE/CVF international conference on computer vision (ICCV), 2019, pp. 6023–6032.
- [16] A. S. Uddin, M. S. Monira, W. Shin, T. C. Chung, S. H. Bae, Saliencymix: A saliency guided data augmentation strategy for better regularization, in: the 9th International Conference on Learning Representations (ICLR), OpenReview.net, 2021.
- [17] E. Georgiou, Y. Avrithis, A. Potamianos, *Powmix*: A versatile regularizer for multimodal sentiment analysis, IEEE/ACM Transactions on Audio, Speech, and Language Processing 32 (2024) 5010–5023.
- [18] S. Venkataramanan, E. Kijak, Y. Avrithis, et al., Embedding space interpolation beyond mini-batch, beyond pairs and beyond examples, in: Advances in Neural Information Processing Systems (NeurIPS), Vol. 36, Curran Associates, Inc., 2023, pp. 61923–61935.
- [19] X. Jin, J. Xiao, L. Jin, X. Zhang, Residual multimodal transformer for expression-ecg fusion continuous emotion recognition, CAAI Transactions on Intelligence Technology 9 (5) (2024) 1290–1304.
- [20] Y. Cimtay, E. Ekmekcioglu, S. Caglar-Ozhan, Cross-subject multimodal emotion recognition based on hybrid fusion, IEEE Access 8 (2020) 168865–168878.
- [21] A. Zadeh, M. Chen, S. Poria, E. Cambria, L.-P. Morency, Tensor fusion network for multimodal sentiment analysis, in: Proceedings of the Conference on Empirical Methods in Natural Language Processing (EMNLP), 2017, pp. 1103–1114.
- [22] Z. Liu, Y. Shen, Efficient low-rank multimodal fusion with modality-specific factors, in: Proceedings of the Association for Computational Linguistics (ACL), Vol. 1, 2018, p. 2247–2256.
- [23] A. Zadeh, P. P. Liang, N. Mazumder, S. Poria, E. Cambria, L.-P. Morency, Memory fusion network for multi-view sequential learning, in: Proceedings of the AAAI conference on artificial intelligence, Vol. 32, 2018.

- [24] F. Lv, X. Chen, Y. Huang, L. Duan, G. Lin, Progressive modality reinforcement for human multimodal emotion recognition from unaligned multimodal sequences, in: Proceedings of the IEEE/CVF conference on computer vision and pattern recognition, 2021, pp. 2554–2562.
- [25] T. Liang, G. Lin, L. Feng, Y. Zhang, F. Lv, Attention is not enough: Mitigating the distribution discrepancy in asynchronous multimodal sequence fusion, in: Proceedings of the IEEE/CVF International Conference on Computer Vision, 2021, pp. 8148–8156.
- [26] D. Yang, S. Huang, H. Kuang, Y. Du, L. Zhang, Disentangled representation learning for multimodal emotion recognition, in: Proceedings of the 30th ACM international conference on multimedia, 2022, pp. 1642–1651.
- [27] R. Lin, H. Hu, Multi-task momentum distillation for multimodal sentiment analysis, *IEEE Transactions on Affective Computing* 15 (2) (2023) 549–565.
- [28] Y. Li, Y. Wang, Z. Cui, Decoupled multimodal distilling for emotion recognition, in: Proceedings of the IEEE/CVF conference on computer vision and pattern recognition, 2023, pp. 6631–6640.
- [29] J.-H. Kim, W. Choo, H. O. Song, Puzzle mix: Exploiting saliency and local statistics for optimal mixup, in: International Conference on Machine Learning (ICML), PMLR, 2020, pp. 5275–5285.
- [30] Z. Liu, S. Li, D. Wu, Z. Liu, Z. Chen, L. Wu, S. Z. Li, Automix: Unveiling the power of mixup for stronger classifiers, in: European Conference on Computer Vision (ECCV), Springer, 2022, pp. 441–458.
- [31] H. Qin, X. Jin, H. Zhu, H. Liao, M. A. El-Yacoubi, X. Gao, Sumix: Mixup with semantic and uncertain information, in: European Conference on Computer Vision (ECCV), Springer, 2024, pp. 70–88.
- [32] X. Jin, H. Zhu, S. Li, Z. Wang, Z. Liu, J. Tian, C. Yu, H. Qin, S. Z. Li, A survey on mixup augmentations and beyond, arXiv preprint arXiv:2409.05202 (2024).
- [33] J. Fu, X. Ji, D. Chen, G. Hu, S. Li, X. Feng, Advmixup: Adversarial mixup regularization for deep learning, *IEEE Transactions on Neural Networks and Learning Systems* (2025).
- [34] V. Verma, A. Lamb, C. Beckham, A. Najafi, I. Mitliagkas, D. Lopez-Paz, Y. Bengio, Manifold mixup: Better representations by interpolating hidden states, in: International Conference on Machine Learning (ICML), PMLR, 2019, pp. 6438–6447.
- [35] L. Sun, C. Xia, W. Yin, T. Liang, P. S. Yu, L. He, Mixup-transformer: Dynamic data augmentation for nlp tasks, in: Proceedings of the International Conference on Computational Linguistics (COLING), 2020, pp. 3436–3440.
- [36] T. Wang, W. Jiang, Z. Lu, F. Zheng, R. Cheng, C. Yin, P. Luo, Vlmixer: Unpaired vision-language pre-training via cross-modal cutmix, in: International Conference on Machine Learning (ICML), PMLR, 2022, pp. 22680–22690.

- [37] R. Lin, H. Hu, Adapt and explore: Multimodal mixup for representation learning, *Information Fusion* 105 (2024) 102216.
- [38] J. Pennington, R. Socher, C. D. Manning, Glove: Global vectors for word representation, in: *Proceedings of the conference on empirical methods in natural language processing (EMNLP)*, 2014, pp. 1532–1543.
- [39] J.-H. Kim, W. Choo, H. O. Song, Puzzle mix: Exploiting saliency and local statistics for optimal mixup, in: *International Conference on Machine Learning (ICML)*, PMLR, 2020, pp. 5275–5285.
- [40] A. Vaswani, N. Shazeer, N. Parmar, J. Uszkoreit, L. Jones, A. N. Gomez, Ł. Kaiser, I. Polosukhin, Attention is all you need, in: *Advances in Neural Information Processing Systems (NeurIPS)*, Vol. 30, Curran Associates, Inc., 2017.
- [41] J. L. Ba, J. R. Kiros, G. E. Hinton, Layer normalization, in: *Advances in Neural Information Processing Systems (NeurIPS)*, Vol. 29, Curran Associates, Inc., 2016, pp. 601–610.
- [42] A. Zadeh, R. Zellers, E. Pincus, L.-P. Morency, Multimodal sentiment intensity analysis in videos: Facial gestures and verbal messages, *IEEE Intelligent Systems* 31 (6) (2016) 82–88.
- [43] A. B. Zadeh, P. P. Liang, S. Poria, E. Cambria, L.-P. Morency, Multimodal language analysis in the wild: Cmu-mosei dataset and interpretable dynamic fusion graph, in: *Proceedings of the Association for computational linguistics (ACL)*, Vol. 1, 2018, pp. 2236–2246.
- [44] W. Yu, H. Xu, F. Meng, Y. Zhu, Y. Ma, J. Wu, J. Zou, K. Yang, Ch-sims: A chinese multimodal sentiment analysis dataset with fine-grained annotation of modality, in: *Proceedings of the Association for Computational Linguistics (ACL)*, 2020, pp. 3718–3727.
- [45] T. Van Erven, P. Harremos, Rényi divergence and kullback-leibler divergence, *IEEE Transactions on Information Theory* 60 (7) (2014) 3797–3820.
- [46] D. Hazarika, R. Zimmermann, S. Poria, Misa: Modality-invariant and-specific representations for multimodal sentiment analysis, in: *Proceedings of the 28th ACM international conference on multimedia*, 2020, pp. 1122–1131.
- [47] A. Zadeh, P. P. Liang, S. Poria, P. Vij, E. Cambria, L.-P. Morency, Multi-attention recurrent network for human communication comprehension, in: *Proceedings of the AAAI conference on artificial intelligence*, Vol. 32, 2018.
- [48] L. v. d. Maaten, G. Hinton, Visualizing data using t-sne, *Journal of machine learning research* 9 (Nov) (2008) 2579–2605.
- [49] P. Foret, A. Kleiner, H. Mobahi, B. Neyshabur, Sharpness-aware minimization for efficiently improving generalization, in: *International Conference on Learning Representations (ICLR)*, 2021.